Available online at www.sciencedirect.com
ScienceDirect
Journal of the European Ceramic Society 28 (2008) 1121–1128
www.elsevier.com/locate/jeurceramsoc

# Effect of initial particle packing on the sintering of nanostructured transition alumina

M. Azar [a], P. Palmero [b], M. Lombardi [b], V. Garnier [a], L. Montanaro [b], G. Fantozzi [a], J. Chevalier [a,*]

[a] *Université de Lyon, INSA-Lyon, MATEIS CNRS UMR 5510, 20 Avenue Albert Einstein, F-69621 Villeurbanne, France*
[b] *Department of Materials Science and Chemical Engineering, Politecnico of Torino, INSTM-UdR PoliTO-LINCE Lab., Torino, Italy*

Received 22 July 2007; received in revised form 20 October 2007; accepted 26 October 2007
Available online 9 January 2008

**Abstract**

The effect of forming method (cold isostatic pressing and slip casting) on particle packing and the consequent effects on densification, phase transformation and microstructural evolution were evaluated during sintering of a transition alumina powder (Nanotek®, particle size of 47 nm, δ and γ phases). It is well known that the transformation of transition alumina towards the stable α phase has a critical influence on the sintering behaviour. Therefore, correlation between microstructural evolution and shrinkage in compacts was established using dilatometry, Scanning Electron Microscopy and X-Ray Diffraction. By the two mentioned forming methods, green bodies with the same density were processed, in order to investigate only particle packing homogeneity and its effect on phase transition and sintering. For the same initial green density, the samples prepared by slip casting present a better homogeneity of particle packing, due to an optimal dispersion of particles in the slurry. This initial microstructure feature improves the particles rearrangement during the transition to α-alumina and hence enhances the transformation to the thermodynamic stable α-phase and the densification step.


*Keywords:* Sintering; Transition alumina; Particle packing; Rearrangement; Slip casting; Cold isostatic pressing

## 1. Introduction

Production of fully dense nanostructured ceramics requires a careful control of each step of ceramic processing, from powder synthesis to the final sintering stage. Moreover, each step may have a detrimental effect on the following one. The effect of forming procedure on particle packing and the consequent effects on sintering have been of paramount importance in the powder processing of ceramics.[1–3]

Furthermore, most nanocrystalline oxide ceramic powders are metastable and this metastability may have a critical influence on the sintering behaviour. Studying the transformation of transition alumina has been the subject of an extensive literature. The transformation proceeds by the formation of several increasingly ordered transition aluminas before final rearrangement into the stable phase α.[4–6] As an example, upon heating, $\gamma$-$Al_2O_3$ undergoes a series of polymorphic phase transformations from a highly disordered cubic close packed lattice to the more ordered cubic close packed $\theta$-$Al_2O_3$. This sequence represents a so-called topotactic deformation. At higher temperatures, $\theta$-$Al_2O_3$ undergoes a reconstructive transformation to form the thermodynamically stable hexagonal close packed α-phase. This transformation occurs by a nucleation and growth process.[6] The transformation into the stable α-$Al_2O_3$ is generally accompanied by vermicular microstructures enclosing a high proportion of intragranular pores. The temperature necessary to remove these pores depends on their size. The production of dense α-$Al_2O_3$ ceramics from transition alumina has been the subject of a considerable number of studies. Most of them were dedicated to the lowering of the phase transformation temperature.[6–11] To our knowledge, less effort was devoted to the lowering of the pore size distribution after the transformation.

Experimental knowledge about phase transformations during the sintering of a compact powder and their dependence to the initial particle packing is important to understand ceramic processing. The aim of this study was therefore to investigate

* Corresponding author. Tel.: +33 4 72 43 61 25; fax: +33 4 72 43 85 28.
*E-mail address:* jerome.chevalier@insa-lyon.fr (J. Chevalier).

0955-2219/$ – see front matter © 2007 Elsevier Ltd. All rights reserved.
doi:10.1016/j.jeurceramsoc.2007.10.003

the effect of forming (slip casting or pressing) on particle packing and its consequent effects on the phase transformations and hence the sintering behaviour of a transition alumina powder.

## 2. Materials and methods

### 2.1. Main features of the nanostructured transition alumina powder

A transition alumina powder produced by Physical Vapor Synthesis (PVS) (NanoTek®, Nanophase Technologies corporation, Romeoville IL, USA) was used in this study. The main features of the as-received powder are summarized in Table 1. Specific surface area was measured using the BET-$N_2$ technique (ASAP 2010 Micromeritics, Norcross, GA) and equivalent spherical diameter calculated from the surface area. True density was measured by pycnometry using He (AccuPyc 1330, Micromeritics, Norcross, GA). The size and morphology of the alumina powder were examined with a Transmission Electron Microscope (JEOL 200 CX, Tokyo, Japan). The crystallographic phases was determined by X-Ray Diffraction (RIGAKU vertical diffractometer, Kent, UK). Fig. 1 shows a Transmission Electron Microscopy (TEM) picture, together with particle size distribution obtained from several images. Fig. 2 represents a X-Ray Diffraction (XRD) pattern of the powder.

In agreement with previous works on the studied powder,[12] the TEM micrograph of Fig. 1a shows that the particles are nearly spherical. The grain size distribution (Fig. 1b), based on the number of particles, shows that the average particle size is around 20 nm and most particles range between 5 and 60 nm. 5% of large particles with size between 60 and 100 nm are present, among them 0.5% with a size close to 150 nm. XRD revealed that the powder consisted of a mixture of δ and γ-alumina. The proportion was evaluated semi-quantitatively from the diffractogramm and from Diffracplus software (Bruker AXS, Madison WI, USA) to be $\delta \approx 70$ wt.% and $\gamma \approx 30$ wt.%. The phase content was in agreement with the data given by the producer.

### 2.2. Forming procedures

Forming of green compacts was conducted via two different methods: dry (pressing) and wet (slip casting) processing methods. Our first objective was to obtain, by the two mentioned forming methods, green bodies with the same density, in order to investigate only particle packing homogeneity and its effect on phase transitions and/or sintering.

Table 1
Main features of the as-received Nanotek® powder

| NanoTEK® aluminum oxide | |
|---|---|
| $Al_2O_3$, white powder | |
| Purity | 99.95% |
| Average particle size (evaluated from SSA) | 47 nm |
| SSA (BET) | 35 $m^2/g$ |
| True density | 3.49 $g/cm^3$ |
| Morphology | Spherical |
| Crystal phase | 70:30; δ:γ |

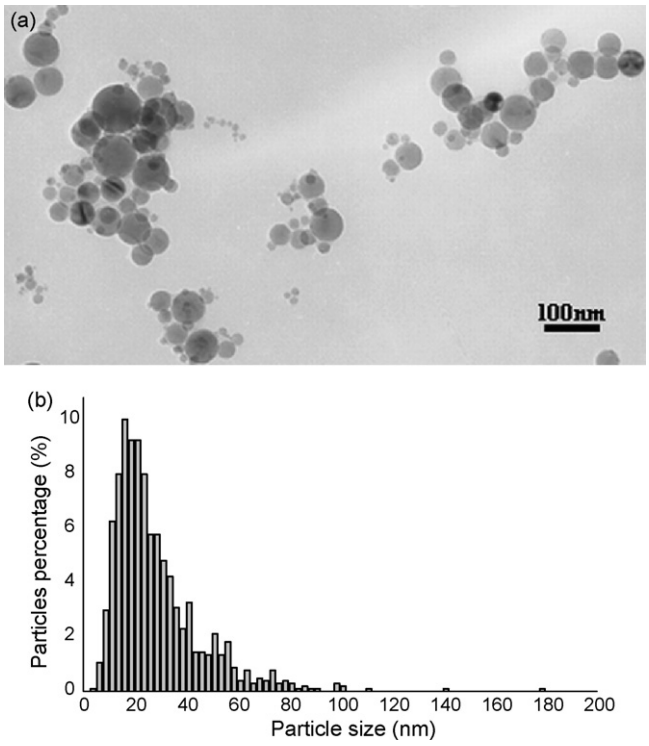


Fig. 1. Transmission Electron Microscopy image (a) and particle size distribution (b) of the Nanotek® powder.

Slip cast specimens (7 mm diameter, 3.5 mm thickness) were prepared from alumina suspensions in distilled water at 22 vol% solid loading. Electrostatic dispersion was achieved using hydrochloric acid. The pH was adjusted to a value of 4.5 (which has been shown to lead to high Zeta potential),[13] and the slurry was stirred for 24 h using 1–2 mm alumina beads (ratio powder: beads of 1:10). The slurries were then cast onto porous alumina molds, in order to avoid contamination of the green body by impurities diffusion. After 24 h, the samples were removed from the mold and put in a dessicator for an additional 24 h.

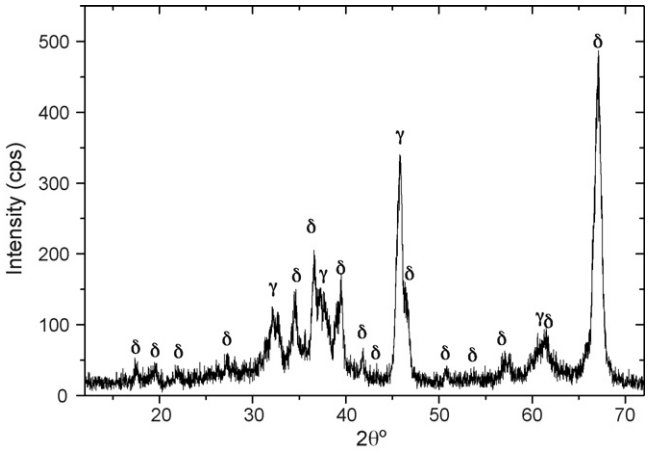


Fig. 2. X-Ray Diffraction pattern of the as received Nanotek® powder.

The density of the green compacts was calculated from mercury porosimetry measurements (Micromeritics Autopore II 9400, Norcross, GA) at the very beginning of the intrusion cycle. With the slip casting conditions mentioned above, green bodies presenting 62% (±1) of the true density (3.49 g/cm$^3$, as measured on the starting powder) were obtained.

To obtain the same (62%) green density, pressed specimens (7 mm diameter, 3.5 mm thickness) were prepared by uniaxial pressing (56 MPa) of the as-received powder followed by Cold Isostatic Pressing (350 MPa). In fact, 62% green density was the maximum value we could obtain by the two methods with this powder.

### 2.3. Follow up of transformation and sintering processes

The transformation and the sintering processes in the alumina compacts were followed with four methods:

- Sintering was conducted in a dilatometer (SETARAM 1700, Caluire, France) up to 1700 °C under non-isothermal conditions in air (heating rate of 5 °C/min and cooling down to room temperature at 20 °C/min). Densities and densification rate curves, as a function of temperature, were computed from the recorded shrinkage data and from the initial densities measured by mercury porosimetry on green samples. Some densification runs were interrupted at different stages of the heat treatment in order to carry out further phase identifications by XRD and microstructural analysis on fractured surfaces by Scanning Electron Microscopy (SEM, FEG XL30, FEI, Eindhoven, Netherlands).
- The thermal behaviour of the compacts was also examined by Differential Thermal Analysis (SETARAM TG-DTA 92, Caluire, France). In particular, Differential Thermal Analysis (DTA) was used to investigate the phase transformation of θ to α-alumina, since the other lower temperature topotactic transformations (i.e. from γ to δ and δ to θ) do not give rise to DTA signal. The compacts were thermally treated to 1500 °C at a heating rate of 5 °C/min in a 20% $N_2$–80% $O_2$ atmosphere and then cooled to room temperature at 20 °C/min.
- XRD (RIGAKU vertical diffractometer, Kent, England) was conducted on the samples heat treated in the dilatometer at different temperatures, to identify the crystalline phases and their evolution versus temperature. XRD patterns were obtained in a $\theta$–$2\theta$ mode, with a Cu Kα radiation. The samples were analysed from $2\theta = 12°$ to 72° at 2°/min for phase identification and from $2\theta = 42°$ to 49° at 0.1°/min for more indepth analysis. The diffractograms were compared to JCPDS files (δ-alumina: ICCD 16-394, γ-alumina: ICDD 50–741, θ-alumina: ICDD 23–1009, α-alumina: ICDD 46–1212). The diffractograms presented in the result section are those conducted between $2\theta = 42°$ and 49°.
- SEM was conducted on the fracture surface of samples heat treated in the dilatometer at different temperatures, to observe the microstructure evolution versus temperature associated to transformation and/or sintering. The samples were gold coated prior to observation (thickness 15 nm), to avoid any surface charge effects even at high magnification and voltage (15 kV). The topography of the samples was imaged under Secondary Electron (SE) mode.

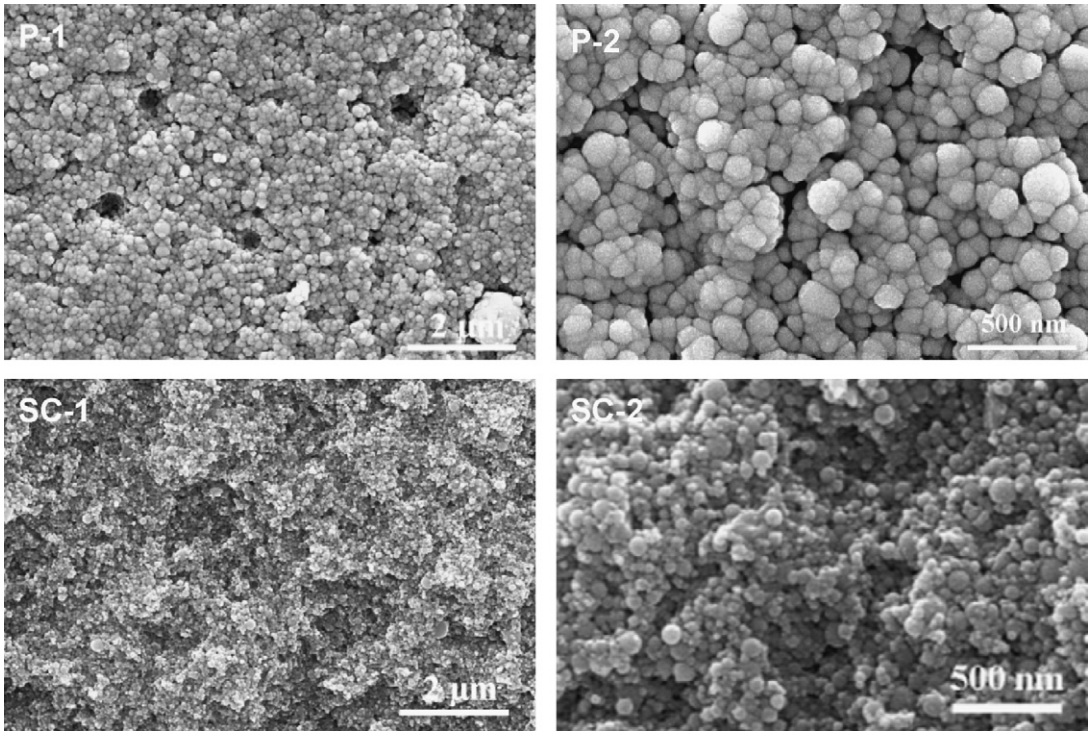


Fig. 3. SEM micrographs of fracture surface for pressed (P-1 and P-2) and slip casted (SC-1 and SC-2) green compacts.

Samples will be noted respect to the forming method (SC for slip casting and P for pressing) and their sintering temperature, for example SC1400 means a slip cast sample sintered at 1400 °C.

## 3. Experimental results and discussion

### 3.1. Effect of forming method on the particle packing

Fig. 3 represents the SEM micrographs of compacts made by pressing and slip casting and having a similar green density. Pressed green compact (P-1, P-2) possess a heterogeneous microstructure with large agglomerates and pores. In fact, the initial powder was agglomerated and forming by dry pressing keeps agglomeration in the green body with formation of two types of pores; inter-agglomerate pores which coexist with smaller intercrystallite pores. Whereas, slip casting method using colloidal suspensions leads to a homogeneous green microstructure (SC-1) because agglomerates have been destroyed, therefore the uniform interparticle pore size increases the packing uniformity (SC-2). This different initial packing can be schematized as in Fig. 4, with a different particle arrangement, for the same number of particles per unit volume.

It is important to note that XRD was conducted on the SC green compacts, in order to verify that they had the same crystallographic phases as those of the initial powder. This means that the milling step used during dispersion does not introduce any transformation to the α phase,[5] and does not produce observable seeding effects,[10,14] (the presence of α seeds can play a key role in the sintering behaviour and enhance the densification of alumina).

### 3.2. Follow up of transformation and sintering processes during non-isothermal heating

Fig. 5 represents the density and densification rate versus temperature. For both types of specimens, the densification

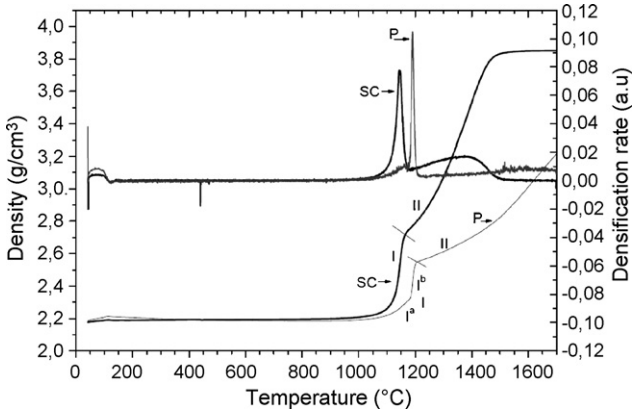


Fig. 5. Density and densification rate versus temperature for SC (slip casted) and P (pressed) specimens.

curve involves two major steps (denoted I and II hereafter). The first step of the densification (up to 1160 or 1200 °C for SC specimens and P specimens, respectively) coincides with the transformation of transition alumina to the thermodynamically stable α-alumina.[14] The second step is associated to the densification of α-alumina. Table 2 summarizes the main features of the two densification steps, for both SC and P specimens. It is to be noted that stage I for P specimens is clearly divided into two 'sub-regions' ($I^a$ and $I^b$), which may correspond to different stage in the transformation process of transition to stable alumina.

Comparing the densification curves of SC and P samples, it can be noticed that:

- Stage I is shifted towards lower temperatures for SC specimens and is accompanied by a larger shrinkage.
- Stage II (densification of α-alumina) is more effective in SC samples. The value of $\rho$ at the end of the sintering run (1700 °C) is 98% for SC1700, while it is only 79% for P1700. Note that final density is reported to the theoretical density of α-$Al_2O_3$ (3.987 g/cm$^3$). A clear maximum of densification rate is even observed for the SC samples (1400 °C), which is

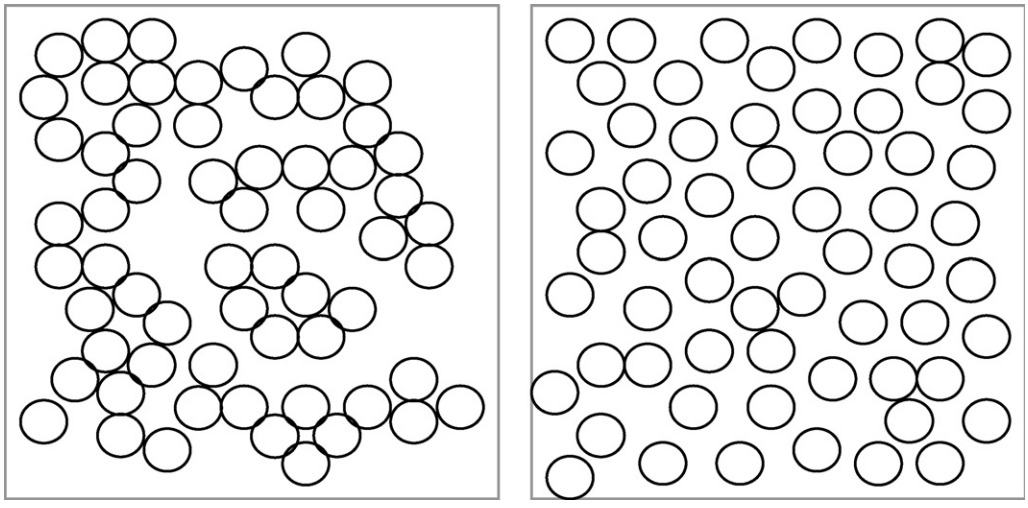

Fig. 4. Schematic illustration of initial particle packing for the green compacts: pressed (left) and slip casted alumina (right).

Table 2
Main features of the densification stages in SC (Slip Casted) and P (pressed) specimens

| | Temperatures at singular points | | | Initial density (g/cm$^3$) | Density at singular point (g/cm$^3$) | $\Delta\rho/\rho$ at singular point | Final density |
|---|---|---|---|---|---|---|---|
| | I | | II | | | | |
| | I$^a$ | I$^b$ | | | | | |
| SC | 1000–1160 °C | | 1160–1700 °C | 2.18 | 2.70 | 24% | 98% |
| P | 1000–1180 °C | 1180–1200 °C | 1200–1700 °C | 2.18 | 2.53 | 16% | 79% |

hardly obtained on transition alumina without any seeding or doping aids.[8,14]

Several samples were prepared at different sintering temperatures in order to observe the evolution of crystallographic phases versus temperature by XRD. Fig. 6 represents the different results obtained on these samples. As reported in other works,[14] stage I of the densification curve correlates with polymorphic transformations of the powder to the α-phase, while only α-alumina is present during stage II. XRD also confirms the difference between SC and P samples in terms of transformation ability, as the compact can be totally converted to α-alumina at 1160 °C for SC or 1200 °C for P. In order to investigate the phase transformation of θ to α-alumina, an observation was carried out using DTA (Fig. 7). The examination of the curves shows that the exothermic reaction occurs at temperatures of 1120 and 1180 °C, respectively, for slip casted and pressed alumina compacts. In fact, the homogeneity of the particle distribution in the slip cast alumina makes easier the rearrangement of the particles as well as reducing the interspacing of the θ particles and increases the number and area of particles contacts. When the particles are brought closer in distance, it makes interaction among the particles easier, thus, bringing about the reduction of the transformation temperature. On the other hand, the temperature of transformation of θ to α of the pressed compact corresponds to the singular point observed in the region I of pressed alumina. The rapid evolution of the relative density in the region I$^b$ (1180–1200 °C) is 9%, near to the variation of the theoretical density from θ to α phase [$(\Delta\rho_R)_{th} = (\rho_\alpha - \rho_\theta)/\rho_\theta = (3.987 - 3.6)/3.6 = 10.75\%$]. We have therefore defined the region I$^b$ as transformation of θ to α.

Considering stage I in general, the crystallographic transformation of transition alumina to α-alumina can not explain by itself the values of density variation observed in Fig. 5. In fact, the relative density variation for the transformation of transition metastable (δ; γ) alumina (3.49 g/cm$^3$) into the stable α-alumina phase (3.987 g/cm$^3$), $(\Delta\rho_R)_{th}$, should be 14.24% [$(\Delta\rho_R)_{th} = (\rho_\alpha - \rho_{\delta;\gamma})/\rho_{\delta;\gamma} = (3.987 - 3.49)/3.49$]. Significant differences in $\Delta\rho_R$ values are observed and depend on

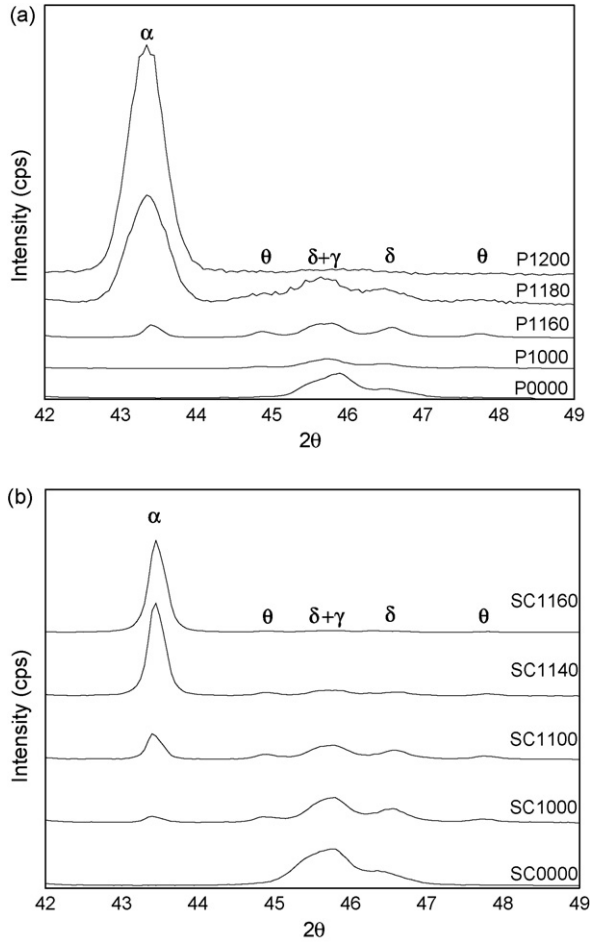


Fig. 6. X-Ray Diffraction patterns of SC and P samples heat treated at different temperatures.

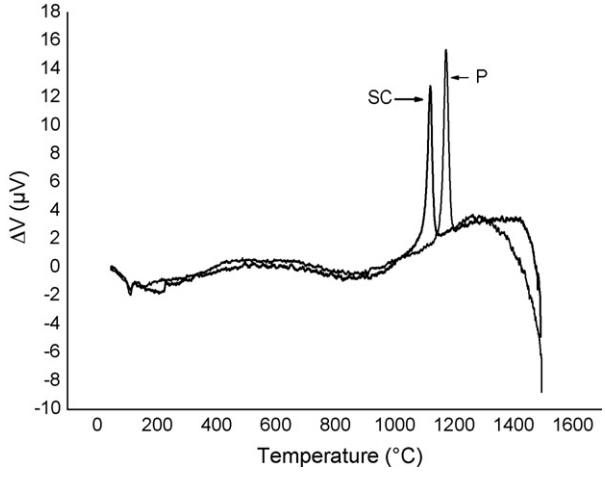


Fig. 7. Differential thermal analysis (DTA) of pressed (P) and slip casted (SC) alumina bodies.

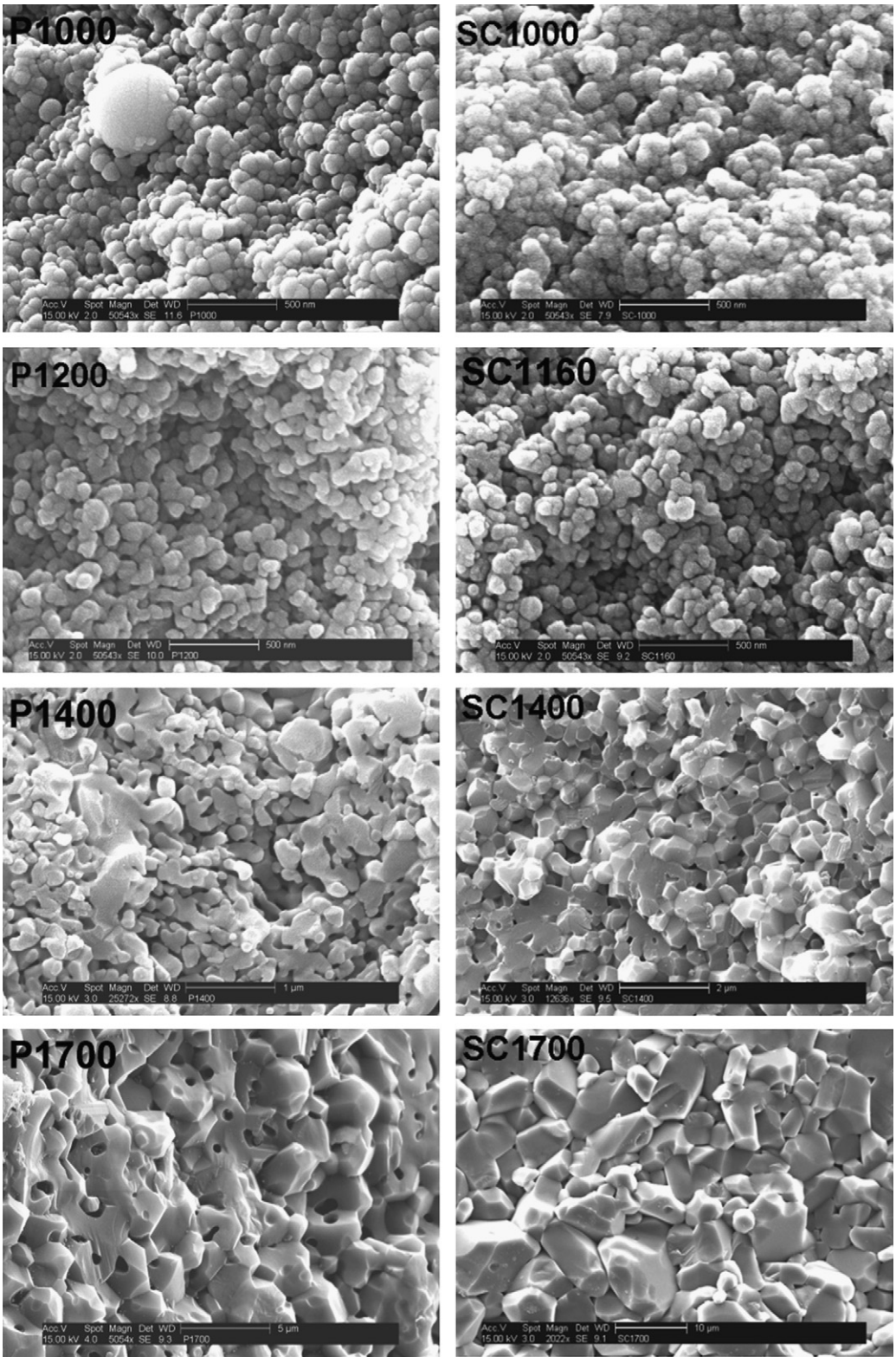


Fig. 8. SEM micrographs of transition alumina sintered at different temperatures.

the forming method: experimental $\Delta\rho_R$ obtained for pressing and slip casting are, respectively, 16 and 24%. These two results are higher than the $(\Delta\rho_R)_{th}$ and it is much marked in the case of slip casting.

Fig. 8 shows SEM micrographs taken on the fracture surface of samples sintered at 1000 °C (before shrinkage), 1160 °C (transition to α-alumina completed for slip casted compact), 1200 °C (transition to α-alumina completed for pressed com-

pact), 1400 °C (densification of α-alumina) and 1700 °C (at the end of sintering).

- At 1000 °C, the microstructure shows almost rounded grains with homogeneous packing for SC1000 but heterogeneous packing with the presence of aggregates for P1000. The linear shrinkage of the pressed and slip casted compacts at this temperature is <1%.
- At 1160 and 1200 °C, respectively, for slip casting and pressing, which correspond to the completion of α-alumina formation, (SC1160 and P1200), SEM also revealed the formation of α colonies consisting of vermicular shaped particles separated by elongated pores. The vermicular colonies were formed by the coalescence of the nuclei during the θ to α transformation instead of growth by grain boundary migration. These results are in good agreement with previous studies for transition alumina.[14] As a result, the $(\Delta\rho_R)_{exp}$ variation from the theoretical values can be explained by the grain rearrangement process coupled with the phase transformation. This rearrangement depends on the initial particle packing. For slip cast alumina, the microstructure of the green compact revealed a uniform distribution of particles and free space is available to the rearrangement of particles. Furthermore, the homogeneous inter particle arrangement would lead to a simultaneous formation of the α-alumina free of vermiculaire growth. While, on pressed compacts, the particles are close packed into agglomerates which make difficult the motion of the particles and decrease the effect of rearrangement. After the transition towards α-phase, the density is 2.7 g/cm$^3$ for slip cast specimens while it is only 2.53 g/cm$^3$ for pressed specimens. The densification of α-$Al_2O_3$, as a consequence, begins at two different densities for pressed and slip casted compacts, despite the same initial green density.
- On the other hand, at 1400 °C, the microstructure of SC1400 is composed of cubeoctahedric grains while for P1400 the microstructure is still porous and vermicular, indicating the higher sintering activity of the slip cast aluminas. The density achieved after a sintering step of 1400 °C is about 90% for the sample made by slip casting while the sample made by pressing had a sintered density of about 67%. In fact, for pressed compacts, the transformations of transition alumina to the stable phase α-alumina have produced large wormy grains enclosing a high proportion of intragranular pores, the elimination of which delays to much higher temperature the elimination of the intracolony porosity. In contrast, homogeneous particle packing in slip cast compacts avoids the formation of wormy crystalline structures with large intragranular pores. Hence, dense material was obtained at lower temperature for the same green density.
- Finally, at 1700 °C, both slip cast and pressed alumina (SC1700 and P1700) present cuboctahedral microstructure with the presence of pores in the case of P1700. Due to the improved sinter activity for slip cast alumina, significant grain growth is observed at 1700 °C leading to a microscaled structure.

## 4. Conclusion

Using two different forming methods, we were able to process green bodies with the same density but different particle packing homogeneity. Initial particle packing plays a significant role on the rearrangement observed during the phase transformation towards α-alumina. Compared to compacts prepared from the pressing of the as received powder, dispersion of the powder and then slip casting improved the homogeneity of particles distribution and hence enhanced the particles rearrangement during the phase transformations into the thermodynamically stable α-phase. This rearrangement produced a drastic change in the microstructural evolution and a significant reduction of the phase transition temperature as well as the quantity and the size of pores remaining after the transition. Therefore, the homogeneous distribution of porosity in the slip cast green compact limits the formation of α-$Al_2O_3$ with hard agglomeration or vermicular morphology and makes sintering to full density easier avoiding formation of large pores that are often entrapped within grains.

## Acknowledgments

The author gratefully acknowledge P. Bowen for fruitful discussions and the European Commission for supporting this work within the framework called “IP NANOKER—Structural Ceramic Nanocomposites for top-end Functional Applications”, contract no.: NMP3-CT-2005-515784. (www.nanoker-society.org).

## References

1. Zheng, J. and Reed, J. S., Effects of particle packing characteristics on solid-state sintering. *J. Am. Ceram. Soc.*, 1988, **72**, 810–817.
2. Nettleship, I. and McAfee, R., Microstructural pathways for the densification of slip cast alumina. *Mater. Sci. Eng.*, 2003, **A352**, 287–293.
3. Dynys, F. W. and Halloran, J. W., Influence of aggregates on sintering. *J. Am. Ceram. Soc.*, 1984, **67**, 596–601.
4. Brindley, G. W., Crystallographic aspects of some decomposition and recrystallisation reactions. In *Progress in Ceramic Science*, *Vol 3*, ed. G. W. Brindley. Pergamon Press, Oxford, 1963, pp. 3–55.
5. Wang, Y., Suryanarayana, C. and An, L., Phase transformation in nanometer-sized γ-alumina by mechanical milling. *J. Am. Ceram. Soc.*, 2005, **88**, 780–783.
6. Yang, X., Pierre, A. C. and Uhlmann, D. R., TEM study of boehmite gels and their transformation to α-alumina. *J. Non-Cryst. Solids*, 1988, **100**, 371–377.
7. Yen, F. S., Wang, M. Y. and Chang, J. L., Temperature reduction of θ to α-phase transformation induced by high-pressure pretreatments of nano-sized alumina powders derived from boehmite. *J. Cryst. Growth*, 2002, **236**, 197–209.
8. Lartigue-Korinek, S., Legros, C., Carry, C. and Herbst, F., Titanium effect on phase transformation and sintering behavior of transition alumina. *J. Eur. Ceram. Soc.*, 2006, **26**, 2219–2230.
9. Wu, Y., Zhang, Y., Pezzotti, G. and Guo, J., Influence of $AlF_3$ and $ZnF_2$ on the phase transformation of gamma to alpha alumina. *Mater. Lett.*, 2002, **52**, 366–369.
10. Kumagai, M. and Messing, G. L., Controlled transformation and sintering of a boehmite sol–gel by α-alumina seeding. *J. Am. Ceram. Soc.*, 1985, **68**, 500–505.

11. Scott Nordahl, C. and Gary, L., Messing: transformation and densification of nanocrystalline θ-alumina during sinter forging. *J. Am. Ceram. Soc.*, 1996, **79**, 3149–3154.
12. Wu, S. J., De Jonghe, L. C. and Rahaman, M. N., Sintering of nanophase γ-$Al_2O_3$ powder. *J. Am. Ceram. Soc.*, 1996, **79**, 2207–2211.
13. Tang, F., Uchikoshi, T., Ozawa, K. and Sakka, Y., Electrophoretic deposition of aqueous nano-γ-$Al_2O_3$ suspensions. *Mater. Res. Bull.*, 2002, **37**, 653–660.
14. Legros, C., Carry, C., Bowen, P. and Hofmann, H., Sintering of a transition alumina: effects of phase transformation, powder characteristics and thermal cycle. *J. Eur. Ceram. Soc.*, 1999, **19**, 1967–1978.